Energy Reports 5 (2019) 271–279

Contents lists available at ScienceDirect

Energy Reports

journal homepage: www.elsevier.com/locate/egyr

Research paper

Improved DTC strategy of doubly fed induction motor using fuzzy logic controller

Najib El Ouanjli [a,*], Saad Motahhir [a], Aziz Derouich [a], Abdelaziz El Ghzizal [a], Ali Chebabhi [b], Mohammed Taoussi [c]

[a] Laboratory of Production Engineering, Energy and Sustainable Development, Higher School of Technology, Sidi Mohamed Ben Abdellah University Fez, Morocco
[b] Faculty of Sciences and Technology, University of Bordj Bou Arreridj, Algeria
[c] Laboratory of Systems Integration and Advanced Technologies, Faculty of Sciences Dhar El Mahraz, Sidi Mohamed Ben Abdellah University Fez, Morocco

ARTICLE INFO

Article history:
Received 17 July 2018
Received in revised form 11 November 2018
Accepted 7 February 2019
Available online xxxx

Keywords:
Direct torque control
Doubly fed induction machine
Fuzzy logic controller
Switching table
Ripple

ABSTRACT

This paper presents an improved Direct Torque Control (DTC) strategy for a Doubly Fed Induction Machine (DFIM) powered by two voltage source inverters (VSI) at two levels. This strategy is based on the fuzzy logic controller. The main objective is to improve the performance of the system by reducing electromagnetic torque ripples and improving the currents shape by optimization of the total harmonic distortion (THD). The hysteresis regulators and voltage vectors selection table of the conventional DTC are replaced by fuzzy logic blocks to realize fuzzy DTC control. The two control strategies are simulated in the MATLAB/SIMULINK environment followed by a comparative analysis to validate the effectiveness of the proposed strategy. Many improvements in term of rise time, torque ripples, flux ripples and current harmonics have been done, namely stator and rotor flux ripple and torque ripple have been reduced more than 50%, 69.2% and 47.7% respectively. The stator and rotor currents THD have been reduced around 84.5% and 84.3% respectively.

1. Introduction

Due to its low cost, simplicity of construction, good performance, reliability, robustness and easy maintenance, the Doubly Fed Induction Machine (DFIM) can provide a very attractive solution especially for variable-speed applications such as wind turbine systems, marine propulsion and electric vehicles (López-Garcıa et al., 2013; Drid et al., 2007; Messalti et al., 2013; Babouri et al., 2013). However, the control of this machine is very complex due to its nonlinearity, its dynamic and the variation of its parameters during operation, as well as it can be exposed to unknown perturbations. Moreover, some of its magnitudes cannot be measured (Bounar et al., 2015). These constraints require more advanced control algorithms to control the torque and flux of this machine in real time (Zemmit et al., 2017). In this regard, several solutions have been developed. The Field Oriented Control (FOC) method was developed to control transient torque (Mehazzem et al., 2017), this command renders the behavior of DFIM similar to that of the DC machine with a decoupling between the torque and the flux (El Ouanjli et al., 2017). This decoupling provides a very fast torque response and a wide speed control range. However, its major disadvantage is the complexity of implementation and sensitivity to parametric variations of the machine (El Ouanjli et al., 2017; Robyns et al., 2000).

Subsequently, Direct Torque Control (DTC) technique is introduced in 1985 by Takahashi and Depenbrock to overcome the problems of vector control (Takahashi and Noguchi, 1986; Depenbrock, 1987). It is characterized by good stability, precision, a fast torque response, high robustness, good decoupling between the torque and flux and low complexity than other controls (El Ouanjli et al., 2017; Telford et al., 2001). This control technique does not require Park transformations, current regulators or specific modulations such as PWM or SVM for pulse generation (Lai and Chen, 2001). However, DTC has major drawbacks namely: (i) The use of hysteresis controllers cause high ripples in the flux and electromagnetic torque that generate mechanical vibrations and undesirable acoustic noise, and therefore, a deterioration of the machine performances (Sutikno et al., 2014). (ii) The variable switching frequency causes switching losses and current distortions that can degrade the quality of the output power (Sutikno et al., 2014; Ammar et al., 2017). (iii) The negligence of stator resistance causes problems at low speed (Casadei et al., 2002).

On the other hand, in recent years, several improvements have been made to enhance the DTC control in order to reduce

* Corresponding author.
E-mail address: najib.elouanjli@usmba.ac.ma (N. El Ouanjli).

https://doi.org/10.1016/j.egyr.2019.02.001

Nomenclature

$v_{s(\alpha,\beta)}$, $v_{r(\alpha,\beta)}$	Stator and rotor voltages in the reference frame (α, β).
$i_{s(\alpha,\beta)}$, $i_{r(\alpha,\beta)}$	Stator and rotor currents in the reference frame (α, β).
$\psi_{s(\alpha,\beta)}$, $\psi_{r(\alpha,\beta)}$	Stator and rotor flux in the reference frame (α, β).
v_a, v_b, v_c	Phase simple voltages.
S_1 , S_2, S_3	Switching states.
R_s, R_r	Stator and rotor resistances.
L_s, L_r	Stator and rotor inductances.
$L\sigma s$, $L\sigma r$	Stator and rotor leakage inductances.
L_m	Mutual inductance.
p	Pole pair number.
ω_s, ω_r	Stator and rotor pulsations.
ω	Mechanical pulsation.
T_r	Load torque.
T_{em}	Electromagnetic torque.
Ω	Rotation speed of the machine.
J	Moment of inertia.
f	Coefficient of viscous friction.
U_c	DC bus voltage.
θ_s, θ_r	Position of the stator and rotor flux.
ε_{Ai}	Error of the magnitude A_i.
$\mu_{(A)}$	Membership function.

Abbreviations

DTC	Direct Torque Control.
DFIM	Doubly Fed Induction Machine.
FLC	Fuzzy Logic Controller.
FOC	Field Oriented Control.
IM	Induction Machine.
MPSM	Permanent Magnet Synchronous Motor.
VSI	Voltage Source Inverter.
THD	Total Harmonics Distortion.

the torque ripple and achieved constant switching frequency. In Flach et al. (1997), Direct Mean Torque Control (DMTC) has been proposed; this method consists in applying two voltage vectors at each sampling period in order to impose an average torque equals to the reference torque. But, the structure of the DMTC is more complicated. Another solution is to use sliding mode control based DTC. However, the chattering phenomenon is the main problem of this method (Lascu et al., 2004). In Jonnala and Babu (2018), the use of multilevel inverters can provide low ripples, but the high number of power devices increases the cost. Therefore, this method is suitable just for high power applications. Alternatively, artificial neural network based DTC can achieve high performance. However, it needs the training process which delays the good performance of the controller (Zemmit et al., 2016).

Therefore, in this work, an intelligent control strategy based on fuzzy logic for the DTC control of a doubly fed induction motor is proposed. The purpose is to minimize the ripples of the torque and flux of the DFIM on the one side and to optimize the Total Harmonic Distortion (THD) of the rotor and stator currents on the other side. The proposed method is constituted of an estimator of stator and rotor flux vectors, an electromagnetic torque estimator and two fuzzy switching tables. The switching laws of the two-level voltage inverter are determined by the linguistic

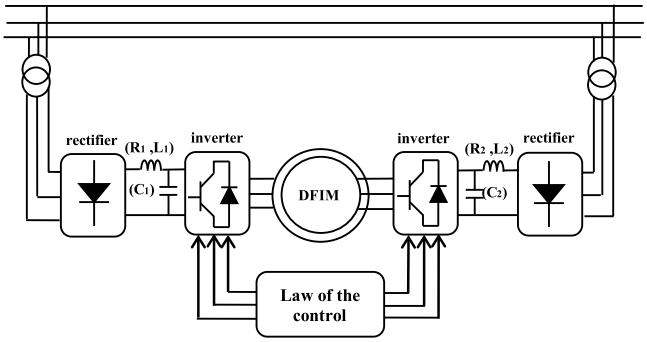

Fig. 1. Overall architecture of the control system of the DFIM.

rules of the fuzzy decision table (Arias et al., 2000). Although many studies about DTC for Induction Motor (IM) and DTC for Permanent Magnet Synchronous Motor (PMSM) using switching tables developed by FLCs have been done individually (Ouledali et al., 2015). However, to the authors best knowledge, no study on fuzzy DTC for DFIM operating in motor mode is available. This gives us the opportunity to design and propose a DTC based on FLC to control DFIM for the first time in the literature. Hence, the main contribution of this work is the effective reduction of torque ripples, flux ripples and THD of the output currents by using a new control method that is robust to variations in DFIM parameters, thus maintaining the advantages of the conventional DTC.

This paper is organized as follows: Section 2 presents the modeling of the doubly fed induction machine and the two-level VSI. Section 3 discusses the conventional DTC technique based on the switch tables and hysteresis controllers. Section 4 discusses the fuzzy DTC strategy based on two fuzzy logic controllers. The simulation results curves using the MATLAB/SIMULINK environment are presented, analyzed and compared in Section 5. Finally, conclusions and suggestions for future works are given in Section 6.

2. Modeling of the system

The power supply of the doubly fed induction machine operating in motor mode and variable speed is assured by two voltage source converters which are mutually connected to the stator and rotor windings (Ourici, 2012). Fig. 1 presents the studied system.

2.1. Dynamic model of DFIM

The most appropriate model to study the dynamic behavior of the DFIM and design of control algorithm is the two-phase model expressed by the coordinates (α, β) (Panchade et al., 2013). This model reduces the complexity of the three-phase representation *(a, b, c)* of the machine.

The equivalent circuit of the DFIM in stator coordinates is depicted in Fig. 2.

The stator voltages equations $v_{s(\alpha,\beta)}$ and the rotor voltages $v_{r(\alpha,\beta)}$ of the DFIM in stator coordinates are expressed by Taoussi et al. (2017):

- Voltages at the stator:

$$\begin{cases} v_{s\alpha} = R_s.i_{s\alpha} + \frac{d\psi_{s\alpha}}{dt} \\ v_{s\beta} = R_s.i_{s\beta} + \frac{d\psi_{s\beta}}{dt} \end{cases} \quad (1)$$

- Voltages at the rotor:

$$\begin{cases} v_{r\alpha} = R_r.i_{r\alpha} + \frac{d\psi_{r\alpha}}{dt} + \omega_m.\psi_{r\beta} \\ v_{r\beta} = R_r.i_{r\beta} + \frac{d\psi_{r\beta}}{dt} - \omega_m.\psi_{r\alpha} \end{cases} \quad (2)$$

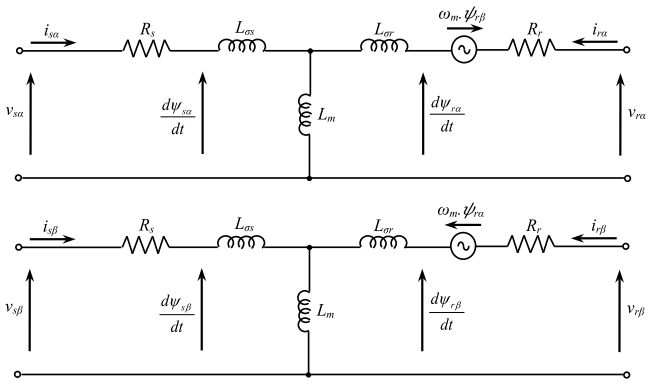

Fig. 2. α β Model of the DFIM in stator coordinates.

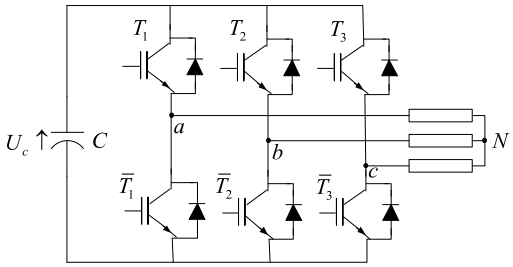

Fig. 3. General structure of the two-level VSI.

With: $\omega_s - \omega_r = \omega_m$

The magnetic equations are defined by the flux expressions in the reference frame (α, β) as follows:

- Flux at the stator:

$$\begin{cases} \psi_{s\alpha} = L_s i_{s\alpha} + L_m . i_{r\alpha} \\ \psi_{s\beta} = L_s i_{s\beta} + L_m . i_{r\beta} \end{cases} \tag{3}$$

- Flux at the rotor:

$$\begin{cases} \psi_{r\alpha} = L_r i_{r\alpha} + L_m . i_{s\alpha} \\ \psi_{r\beta} = L_r i_{r\beta} + L_m . i_{s\beta} \end{cases} \tag{4}$$

With: $L_s = L_{\sigma s} + L_m$ *and* $L_r = L_{\sigma r} + L_m$

The electromagnetic torque expression of DFIM as a function of the stator flux and the stator currents is written as follows:

$$T_{em} = p.(\psi_{s\alpha} i_{s\beta} - \psi_{s\beta} i_{s\alpha}) \tag{5}$$

The fundamental equation of dynamics is:

$$J.\frac{d\Omega}{dt} + f.\Omega = T_{em} - T_r \tag{6}$$

2.2. Modeling of the voltage source inverter

The purpose of voltage inverter modeling is to find a relation between the control variables and the electrical variables of the AC and DC part of this inverter.

The general structure of the two-level VSI is shown in Fig. 3. It is composed of two switches (IGBT) in each arm.

The mathematical model of the two-level VSI is represented by the following matrix:

$$\begin{bmatrix} v_a \\ v_b \\ v_c \end{bmatrix} = \frac{U_c}{3}.\begin{bmatrix} 2 & -1 & -1 \\ -1 & 2 & -1 \\ -1 & -1 & 2 \end{bmatrix}.\begin{bmatrix} S_1 \\ S_2 \\ S_3 \end{bmatrix} \tag{7}$$

The switches state supposed to be perfect. It can be represented by three Boolean magnitudes of command $S_i (i = 1, 2$ and $3)$, such as:

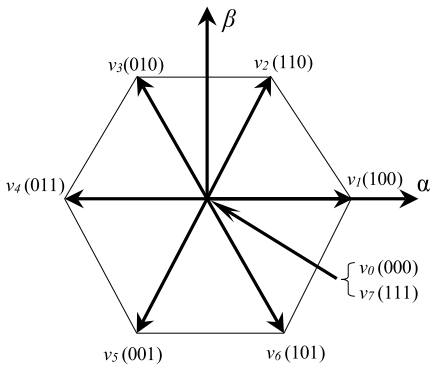

Fig. 4. Voltage vectors delivered by the inverter.

- $S_i = 1$ if T_j is closed and $\overline{T}_j$ is open.
- $S_i = 0$ if T_j is open and $\overline{T}_j$ is closed.

With $(j = 1, 2, 3)$.

3. Direct torque control

The direct torque control consists in controlling the opening or closing of switches of two voltage source inverters by the direct determination of control sequence applied to these switches (El Ouanjli et al., 2017; Ouanjli et al., 2017). This choice is generally based on the use of hysteresis controllers whose the function is to control the electromagnetic torque and the magnitude of flux (El Mourabit et al., 2017), it is required to keep these two magnitudes in the defined error ranges. The two outputs of the controllers are combined with the position of the flux vector to determine the switching table of the inverter control (Casadei et al., 2002).

The vector voltage expression of each two-level VSI can be given in the form below:

$$V = \sqrt{(2/3)}.U_0.(S_1 + S_2 e^{(j2\pi/3)} + S_3 e^{(j4\pi/3)}) \tag{8}$$

Fig. 4 presents the set of voltage vectors delivered by each inverter:

The direct torque control of the DFIM relies mainly on the estimation of the magnitudes to be controlled, namely the electromagnetic torque, the stator flux and the rotor flux.

The stator flux vector is estimated from the measurements of the voltages and currents of the DFIM. The expression of the stator flux is written:

$$\begin{cases} \hat{\psi}_{s\alpha} = \int_0^t (v_{s\alpha} - R_s . i_{s\alpha}) \, .dt \\ \hat{\psi}_{s\beta} = \int_0^t \left(v_{s\beta} - R_s . i_{s\beta}\right) .dt \end{cases} \tag{9}$$

With: $\overline{\psi}_s = \hat{\psi}_{s\alpha} + j\hat{\psi}_{s\beta}$

The modulus of stator flux is written:

$$\hat{\psi}_s = \sqrt{\hat{\psi}_{s\alpha}^2 + \hat{\psi}_{s\beta}^2} \tag{10}$$

The sector S_i in which one is situated the vector ψ_s was determined from the components $\psi_{s\alpha}$ and $\psi_{s\beta}$. The angle θ_s between the referential linked to the stator and the vector ψ_s is equal to:

$$\theta_s = arctg(\frac{\hat{\psi}_{s\beta}}{\hat{\psi}_{s\alpha}}) \tag{11}$$

The same way for the case of the rotor flux is followed:

$$\hat{\psi}_r = \sqrt{\hat{\psi}_{r\alpha}^2 + \hat{\psi}_{r\beta}^2} \tag{12}$$

Table 1
Switching table.

		Sector S_i					
		1	2	3	4	5	6
$H_{\psi s}$or $H_{\psi r}$	H_{Tem}	Voltage vector					
1	1	v_2	v_3	v_4	v_5	v_6	v_1
	0	v_7	v_0	v_7	v_0	v_7	v_0
	−1	v_6	v_1	v_2	v_3	v_4	v_5
0	1	v_3	v_4	v_5	v_6	v_1	v_2
	0	v_0	v_7	v_0	v_7	v_0	v_7
	−1	v_5	v_6	v_1	v_2	v_3	v_4

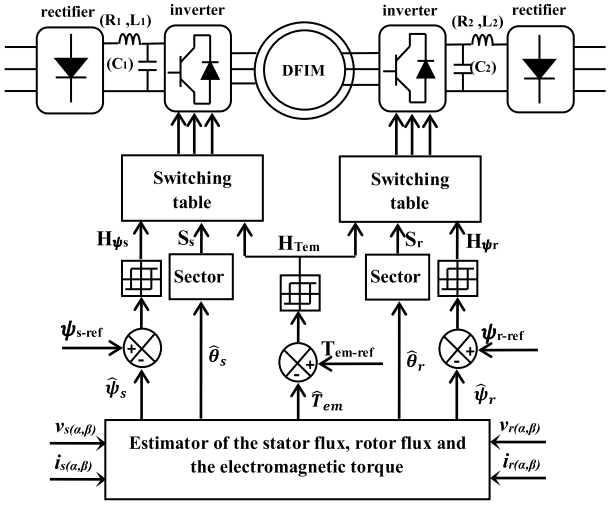

Fig. 5. Synoptic schema of the conventional DTC.

$$\theta_r = arctg\left(\frac{\hat{\psi}_{r\beta}}{\hat{\psi}_{r\alpha}}\right) \tag{13}$$

The electromagnetic torque is estimated from the measured rotor currents:

$$T_{em} = p.(\psi_{r\alpha} i_{r\beta} - \psi_{r\beta} i_{r\alpha}) \tag{14}$$

The error ε_ψ between the reference flux ψ_{ref} and estimated flux $\hat{\psi}$ is introduced into a two-level hysteresis regulator, the latter will generate the binary variable ($H_\psi = 0, 1$) at its output, representing the desired evolution for the flux. Similarly, the immediate error of the torque ε_{Tem} is calculated by comparing its reference value T_{em-ref} and its estimated value $\hat{T}_{em}$, then applied to a three-level hysteresis regulator, generating at its output the variable H_{Tem} with three levels (−1, 0, 1), representing the direction of temporal evolution desired for the torque.

The state choice of each VSI is made in a switching table elaborated according to the state of the variables H_ψ and H_{Tem}, as well as sector giving the information about the position of flux vector (Ouanjli et al., 2017).

The switching table is presented in Table 1:

The general structure of conventional DTC applied to the doubly fed induction motor is illustrated by the following Fig. 5:

4. Direct torque control based on fuzzy logic

To improve the performances of the system and to minimize ripples in the electromagnetic torque and flux, two fuzzy logic controllers are used to replace the controllers of hysteresis and the conventional switching tables. In this system, flux error, torque error and flux angle are considered as inputs to each fuzzy logic controller.

$$\varepsilon_{\psi s} = \psi_{s-ref} - \hat{\psi}_s = \Delta\psi_s \tag{15}$$

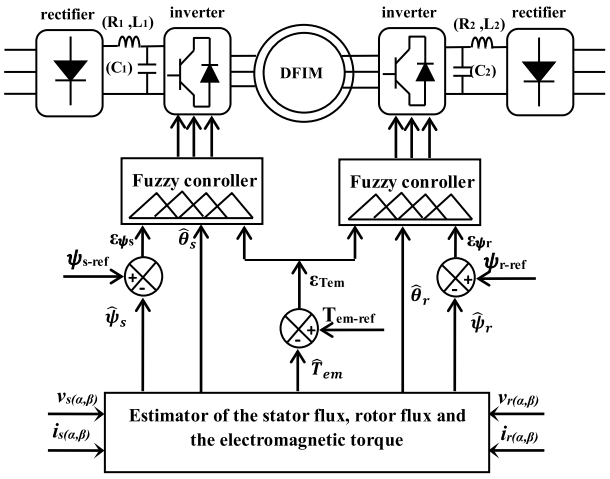

Fig. 6. Synoptic schema of the fuzzy DTC.

$$\varepsilon_{\psi r} = \psi_{r-ref} - \hat{\psi}_r = \Delta\psi_r \tag{16}$$

$$\varepsilon_{Tem} = T_{em-ref} - \hat{T}_{em} = \Delta T_{em} \tag{17}$$

These error functions are the differences between a magnitude calculated from the information provided by the command and the estimated magnitude. Each input is divided into a determined number of fuzzy sets so as to have a better control using the minimum of rules.

Fig. 6 presents the block diagram adopted for fuzzy DTC control of the doubly fed induction motor.

Generally, the control by fuzzy logic is done in three steps: fuzzification, the use of rules table to determine the output based on inputs and the defuzzification (Akın et al., 2003).

4.1. Inputs fuzzification

The aim of fuzzification process is to transform the deterministic input variables into linguistic variables by defining membership functions for each input variables.

The first input variable is the flux position (stator or rotor flux). The discourse universe of this variable is composed of six fuzzy sets (θ_1 to θ_6) whose membership functions are represented in Fig. 7.

The triangular membership function is chosen for all angles θ_i.

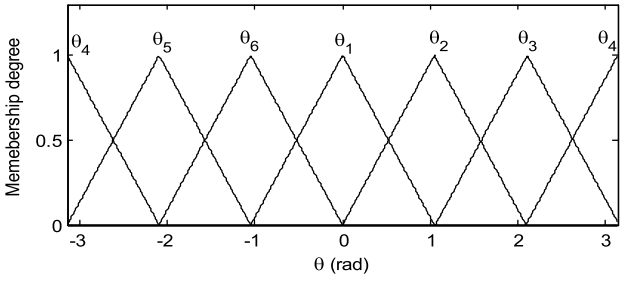

Fig. 7. Membership function for flux position.

The second input is the error of electromagnetic torque, its universe of discourse is composed of three fuzzy sets:

- Torque error is positive (P);
- Torque error is zero (Z);
- Torque error is negative (N).

Fig. 8 shows the trapezoid membership functions for the two fuzzy sets (P) and (N) and the triangular membership function for the fuzzy set (Z).

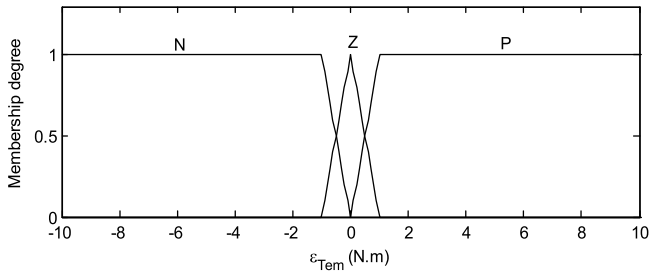

Fig. 8. Membership function for electromagnetic torque error.

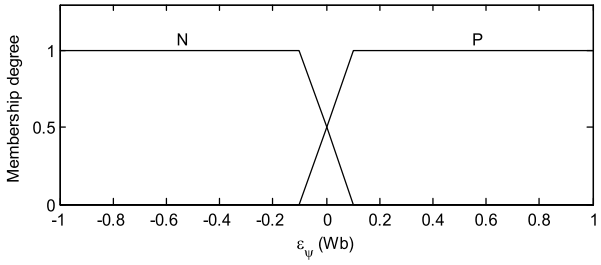

Fig. 9. Membership function for flux linkage error.

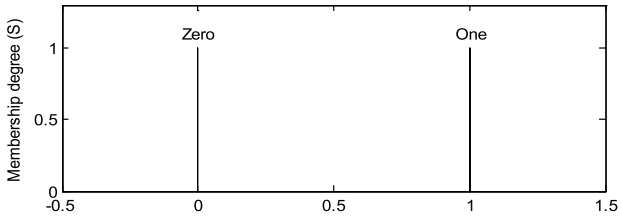

Fig. 10. Membership functions for output variables.

The third input variable is the flux error; its universe of discourse is divided into two fuzzy sets:

- Flux error is positive (P);
- Flux error is negative (N);

As shown in Fig. 9, the trapezoid membership function is chosen for the two fuzzy sets.

4.2. Outputs defuzzication

This step consists in transforming the fuzzy information established by the inference mechanism into a physical or numerical magnitude to define the control law of the process.

The output variable is composed of three sub-outputs representing three switching magnitudes (S_1, S_2 S_3) of the inverter switches, the universe of discourse of each output is divided into two fuzzy sets (zero and one) whose membership functions are chosen by trapezoid forms represented in Fig. 10.

4.3. Control rules

The control rules must be designed according to the input and output variables based on the conventional DTC switching table. The structure of fuzzy logic controller is represented by Fig. 11.

The fuzzy rules for determining the output variables of the controller according to the input variables are grouped in Table 2:

The control algorithm has 36 rules, the inference method used is the Mamdani method based on the Max–Min decision due to its low complexity to be implemented on the one hand and it gives better results on the other hand, this method is expressed by:

$$\mu_{Ri} = \min\left(\mu_{Xi}(\varepsilon_{\theta}), \mu_{Yi}(\varepsilon_{Tem}), \mu_{Wi}(\varepsilon_{\psi})\right) \quad (18)$$

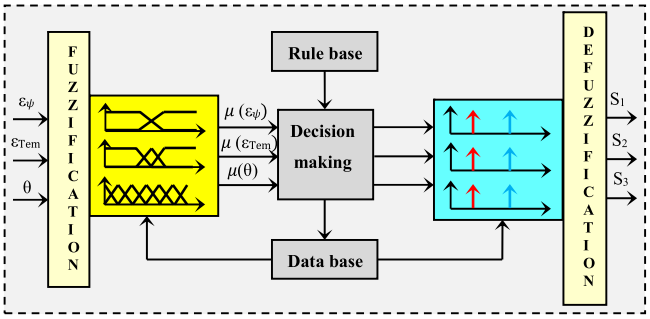

Fig. 11. Structure of the fuzzy controller for the two-level inverter.

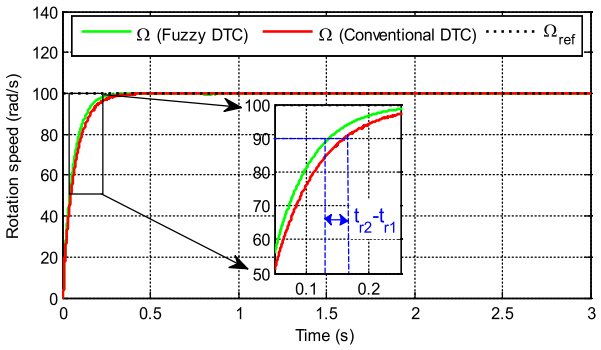

Fig. 12. Rotation speed.

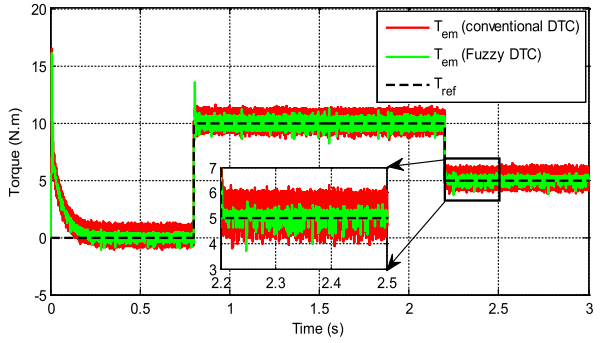

Fig. 13. Electromagnetic torque.

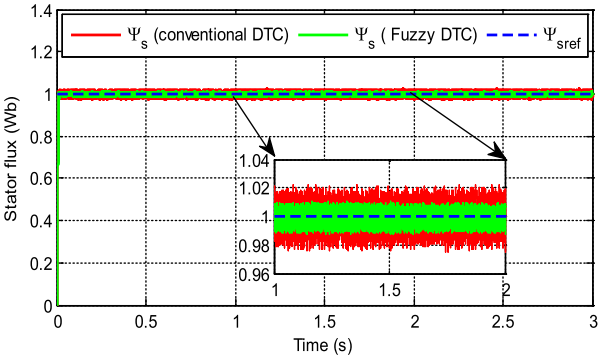

Fig. 14. Stator flux.

Table 2
Set of fuzzy rules.

θ_1			
e_{Tem} / e_ψ	N	Z	P
N	v_5	v_0	v_3
P	v_6	v_7	v_2

θ_2			
e_{Tem} / e_ψ	N	Z	P
N	v_6	v_7	v_4
P	v_1	v_0	v_3

θ_3			
e_{Tem} / e_ψ	N	Z	P
N	v_1	v_0	v_5
P	v_2	v_7	v_4

θ_4			
e_{Tem} / e_ψ	N	Z	P
N	v_2	v_7	v_6
P	v_3	v_0	v_5

θ_5			
e_{Tem} / e_ψ	N	Z	P
N	v_3	v_0	v_1
P	v_4	v_7	v_6

θ_6			
e_{Tem} / e_ψ	N	Z	P
N	v_4	v_7	v_2
P	v_5	v_0	v_1

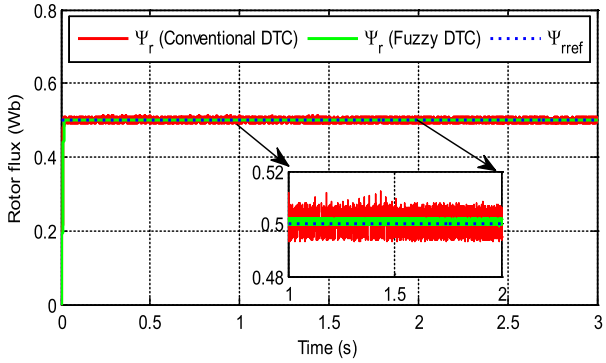

Fig. 15. Rotor flux.

By the fuzzy reasoning, Mamdani minimum process gives:

$$\mu_{N'i} = \min\left(\mu_{ri}, \mu_{Ni}(n)\right) \tag{19}$$

The membership function μ_N of the output is then given by:

$$\mu_N(n) = \max\left(\mu_{N'i}(n)\right), i = 1, 2, \ldots..36. \tag{20}$$

The control rules are expressed as a function of the input and output variables as follows:

If (θ is X) and (ε_{Tem} is Y) and (ε_ψ is W) then (V is V_i).

Where X, Y and W are the fuzzy set of the input variables, $V_i(S_1, S_2, S_3)$ the fuzzy set of the output variables.

Examples of the control rule:

- If (θ is θ_1) and (ε_{Tem} is P) and (ε_ψ is P) then (S_1 is 0) and (S_2 is 1) and (S_3 is 0).
- If (θ is θ_2) and (ε_{Tem} is N) and (ε_ψ is P) then (S_1 is 1) and (S_2 is 0) and (S_3 is 1).

5. Simulation results and discussion

In this section, the conventional and fuzzy torque direct control applied to the doubly fed induction machine functioning in motor mode of 1,5 kW (its parameters are given in the Appendix) powered by two voltage inverters at two-level were tested by simulation in MATLAB/SIMULINK environment. The main features of this simulation are summarized as follows:

- The widths of the hysteresis bands: $\Delta_{Tem} = \pm 0.01$ N.m, $\Delta_{\psi s} = \pm 0.001$ N.m and $\Delta_{\psi r} = \pm 0.001$ N.m.
- The sampling frequency $f_s = 10$ kHz.
- DC bus voltages: $U_{dc-s} = 300$ V et U $_{dc-r} = 100$ V.
- The machine is started without load for 0.8s.
- By applying a load torque of 10 N.m and 5 N.m respectively to $t_1 = 0.8$ s and $t_2 = 2.2$ s.

The simulation results are presented in the figures below:

- Figs. 12 and 13 show that the rotation speed and electromagnetic torque of the machine follow its references, with a very fast speed response time which is around 0.28 s and a reduced rise time in the fuzzy DTC control compared to the conventional DTC control. Moreover, it is clear that the load torque impacts do not affect the system speed response for both control techniques.
- Figs. 14 and 15 show that the modulus of the stator and rotor flux vector follows perfectly the reference flux (1Wb for stator flux and 0.5Wb for rotor flux).
- The electromagnetic torque and flux of the machine in the case of the fuzzy DTC present low oscillations compared to the conventional DTC control. Similarly, the trajectory of the stator and rotor flux has a fine circular shape compared to that obtained by the conventional DTC (Fig. 16). It is also noted that the variation of the torque has no influence on the flux, which shows that there is a decoupling between the torque and the flux.

These results show clearly the robustness of the fuzzy DTC control and an apparent reduction of the ripples brought from the torque and the flux.

- Figs. 17 and 19 present respectively the components of the stator and rotor currents in the frame (a,b,c) which have sinusoidal patterns with a frequency proportional to the reference speed, they respond effectively to the variations imposed by the load torque.
- Figs. 18 and 20 show respectively the analysis of the harmonic spectra for the phase "a" of the stator and rotor current absorbed by the DFIM. It is shown that the total harmonic distortion (THD) of the currents by the fuzzy DTC control is considerably reduced compared to the conventional DTC.

It is well recognized that the THD in the currents is heavily influenced by the ripples in torque and flux, a good regulation of torque and flux optimizes the THD and improves the quality of the output power, which is also observable in the results presented. The fuzzy DTC offers a significant reduction in THD when compared to the conventional DTC.

The Table 3 below presents a synthesis of comparison between the fuzzy DTC and conventional DTC in term of the rise time, torque ripples, stator and rotor flux ripples and currents harmonic. This table shows remarkable improvements obtained by fuzzy DTC. These improvements include an optimization of the rise time, an important reduction in ripples of torque and flux, as well as a minimization in the harmonics of the stator and rotor current signals. Therefore, the proposed method provides better performance compared to conventional DTC.

Table 4 shows a Comparison between the proposed technique and some controls strategy published recently. It should be mentioned that they do not refer to the same conditions since

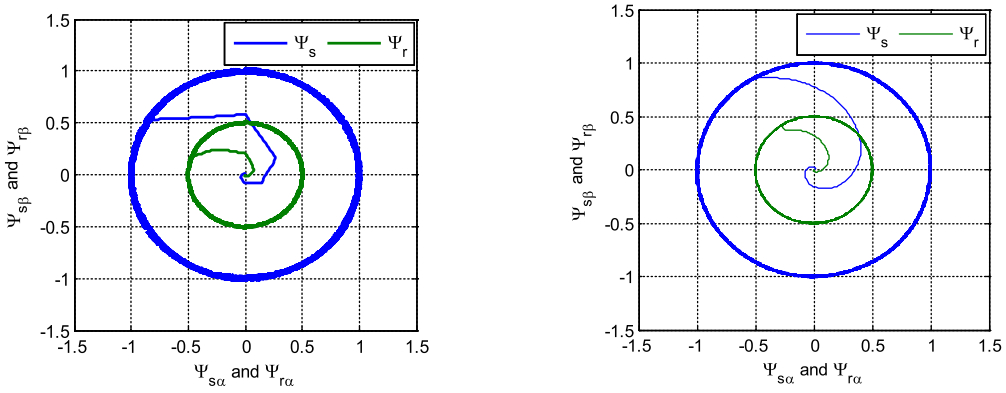

Fig. 16. Evolution of the stator and rotor flux by the control: (a) Conventional DTC (b) Fuzzy DTC.

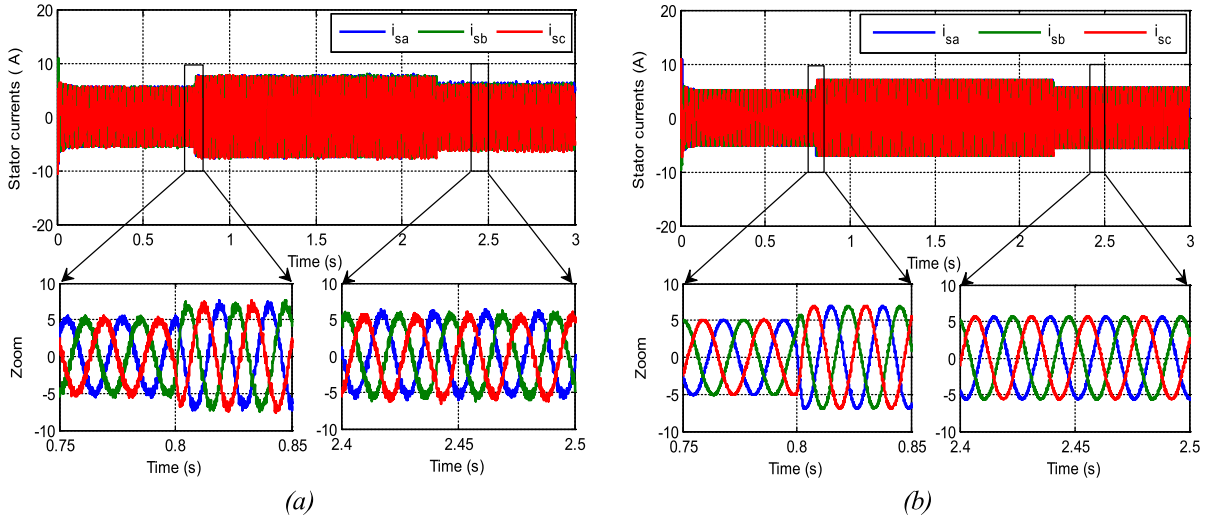

Fig. 17. Stator currents by the control: (a) Conventional DTC (b) Fuzzy DTC.

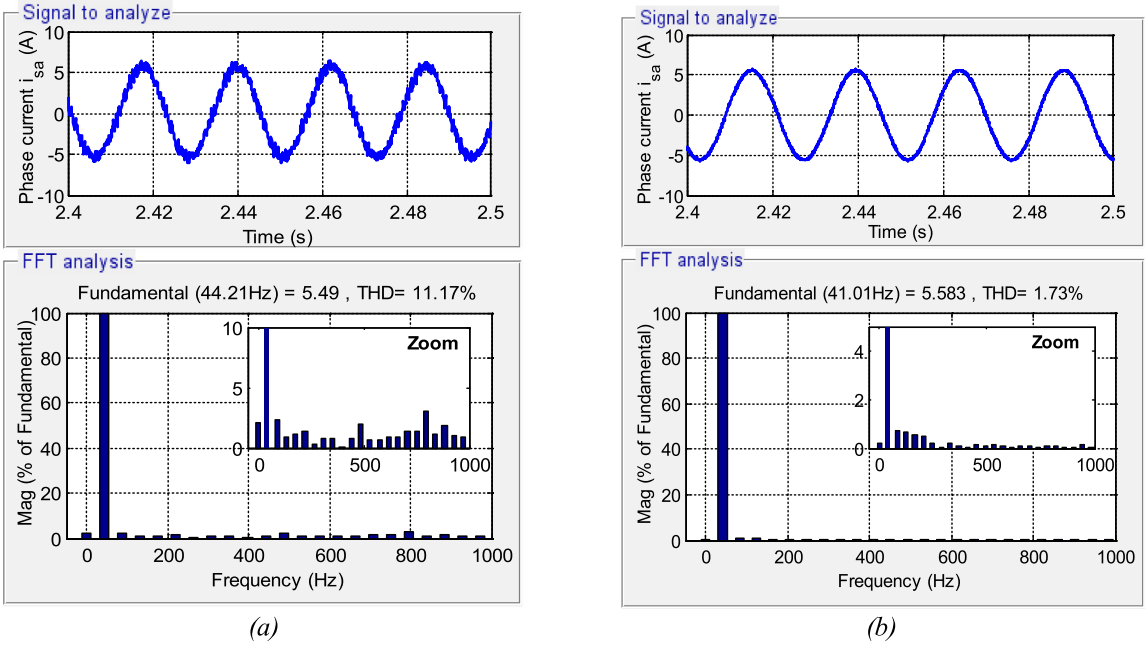

Fig. 18. Harmonic analysis of stator current spectra by control: (a) Conventional DTC (b) Fuzzy DTC.

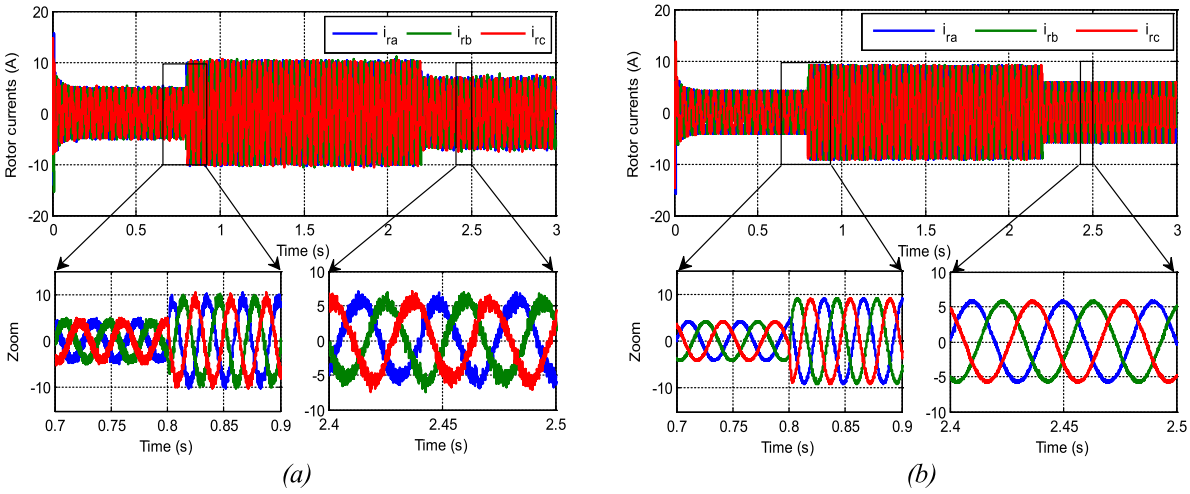

Fig. 19. Rotor currents by the control: (a) Conventional DTC (b) Fuzzy DTC.

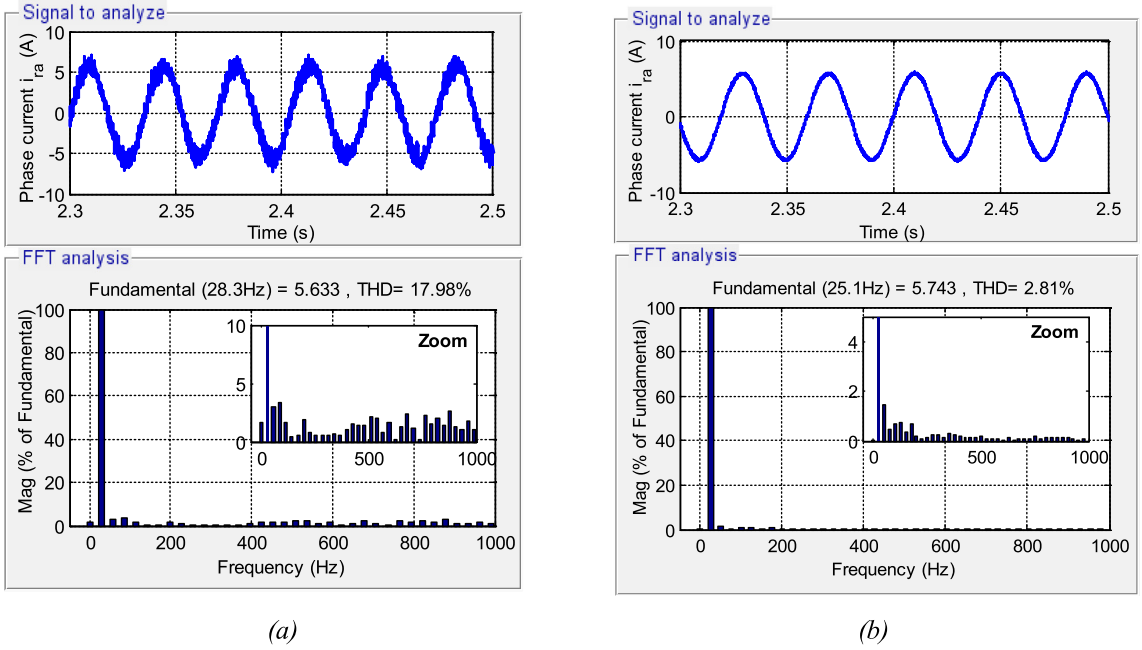

Fig. 20. Harmonic analysis of rotor current spectra by control: (a) Conventional DTC (b) Fuzzy DTC.

Table 3
Comparative results between conventional DTC and fuzzy DTC.

Performance	Conventional DTC	Fuzzy DTC	Improvement (%)
Rise time of the speed (s)	0.162	**0.133**	**17.9**
Torque ripple (N.m)	2.18	**1.14**	**47.7**
Stator flux ripple (Wb)	0.04	**0.02**	**50**
Rotor flux ripple (Wb)	0.013	**0.004**	**69.2**
THD of the phase current i_{sa} (%)	11.17	**1.73**	**84.5**
THD of the phase current i_{ra} (%)	17.98	**2.81**	**84.3**

it is very difficult to find several works done under the same conditions. So if the proposed work is compared with FOC and conventional DTC (El Ouanjli et al., 2017; Abdellatif et al., 2014), our solution presents a faster response, significant reduction in torque ripples as well as a reduction in the ripples of flux and currents. Thus, the sliding mode control presented by Abderazak and Farid (2016) has larger torque ripples than our proposal. Moreover, our system is insensitive to variations in load torque, which shows a high level of robustness. Consequently, the fuzzy DTC provides a good static and dynamic performance of the machine studied.

6. Conclusion

In this paper, a new fuzzy logic direct torque control scheme of doubly fed induction motor powered by two voltage source inverters was introduced, the objective is to improve the DTC performance. The modeling of DFIM and details of DTC strategy

Table 4
Comparison between our proposal and some controls strategy published recently.

Publication year, Paper	Technique	Response time (s)	Rise time (s)	Torque ripple (N.m)	Control variable	robustness
El Ouanjli et al. (2017)	Field Oriented Control	0.56	0.18	2.50	Current I	Not robust
Abderazak and Farid (2016)	Sliding mode control	0.19	0.112	2.40	Current I	Not robust
Abdellatif et al. (2014)	Conventional Direct Torque Control	0.32	0.162	2.18	Flux ψ and torque T_{em}	robust
Proposal method	Fuzzy Direct Torque control	0.28	0.113	1.14	Flux ψ and torque T_{em}	robust

Table A.1
Parameters of the DFIM.

Variable	Symbol	Value (unit)
Nominal power	P_n	1.5 kW
Stator nominal voltage	V_{sn}	230 V
Rotor nominal voltage	V_{rn}	130 V
Frequency	f	50 Hz
Pair pole number	P	2
Stator self-inductance	Ls	0.295 H
Rotor self-inductance	Lr	0.104 H
Maximum of mutual inductance	M	0.165 H
Stator resistance	R_s	1.75 Ω
Rotor resistance	R_r	1.68 Ω
Total viscous frictions	f	0.0027 kg.m^2/s
Total inertia	J	0.01 kg.m^2

have been presented. The control strategy DTC based on fuzzy logic controllers is developed in detail. After testing the system controls using MATLAB/SIMULINK, the key findings of this work are as follows:

- Fuzzy logic controller provides effective DTC improvements, the torque and flux ripples are reduced, consequently fewer problems for the motor (heating, mechanical vibration, aging …).
- The robustness and fast response merits of the conventional DTC are preserved.
- The good regulation of torque and flux by the FLC improve the harmonic distortion in stator and rotor currents.

The future work will address the experimental implementation of the proposed method and to develop a hybrid model having the various methods of improvement of control strategy studied.

Appendix

See Table A.1.

References

Abdellatif, M., Debbou, M., Slama-Belkhodja, I., Pietrzak-David, M., 2014. Simple low-speed sensorless dual DTC for double fed induction machine drive. IEEE Trans. Ind. Electron. 61 (8), 3915–3922.

Abderazak, S., Farid, N., 2016, December. Comparative study between Sliding mode controller and Fuzzy Sliding mode controller in a speed control for doubly fed induction motor. In: IEEE 4th International Conference in Control Engineering & Information Technology, pp. 1–6.

Akın, E., Kaya, M., Karakose, M., 2003. A robust integrator algorithm with genetic based fuzzy controller feedback for direct vector control. Comput. Electr. Eng. 29 (3), 379–394.

Ammar, A., Bourek, A., Benakcha, A., 2017. Nonlinear SVM-DTC for induction motor drive using input–output feedback linearization and high order sliding mode control. ISA Trans. 67, 428–442.

Arias, A., Romeral, J.L., Aldabas, E., Jayne, M.G., 2000, December. Fuzzy logic direct torque control. In: Proceedings of the 2000 IEEE International Symposium In Industrial Electronics, vol. 1, pp. 253–258.

Babouri, R., Aouzellag, D., Ghedamsi, K., 2013. Introduction of doubly fed induction machine in an electric vehicle. Energy Procedia 36, 1076–1084.

Bounar, N., Boulkroune, A., Boudjema, F., Farza, M., 2015. Adaptive fuzzy vector control for a doubly-fed induction motor. Neurocomputing 151, 756–769.

Casadei, D., Profumo, F., Serra, G., Tani, A., 2002. FOC and DTC: two viable schemes for induction motors torque control. IEEE Trans. Power Electron. 17 (5), 779–787.

Depenbrock, M., 1987, June. Direct self-control (DSC) of inverter fed induktion machine. In: IEEE Power Electronics Specialists Conference, pp. 632–641.

Drid, S., Tadjine, M., Naït-Saïd, M.S., 2007. Robust backstepping vector control for the doubly fed induction motor. IET Control Theory Appl. 1 (4), 861–868.

El Mourabit, Y., Derouich, A., El Ghzizal, A., El Ouanjli, N., Zamzoum, O., 2017. DTC-SVM Control for permanent magnet synchronous generator based variable speed wind turbine. Intl. J. Power Electron. Drive Syst. 8 (4), 1732–1743.

El Ouanjli, N., Derouich, A., El Ghzizal, A., Chebabhi, A., Taoussi, M., 2017, November. A comparative study between FOC and DTC control of the Doubly Fed Induction Motor (DFIM). In: IEEE International Conference In Electrical and Information Technologies, ICEIT, pp. 1–6.

Flach, E., Hoffmann, R., Mutschler, P., 1997. Direct mean torque control of an induction motor. In: European Conference on Power Electronics and Applications, vol. 3. Proceedings published by various publishers, pp. 3–672.

Jonnala, R.B., Babu, C.S., 2018. A modified multiband hysteresis controlled DTC of induction machine with 27-level asymmetrical CHB-MLI with NVC modulation. Ain Shams Eng. J. 9 (1), 15–29.

Lai, Y.S., Chen, J.H., 2001. A new approach to direct torque control of induction motor drives for constant inverter switching frequency and torque ripple reduction. IEEE Trans. Energy Convers. 16 (3), 220–227.

Lascu, C., Boldea, I., Blaabjerg, F., 2004. Direct torque control of sensorless induction motor drives: a sliding-mode approach. IEEE Trans. Ind. Appl. 40 (2), 582–590.

López-Garcıa, I., Espinosa-Pérez, G., Siguerdidjane, H., Dòria-Cerezo, A., 2013. On the passivity-based power control of a doubly-fed induction machine. Int. J. Electr. Power Energy Syst. 45 (1), 303–312.

Mehazzem, F., Nemmour, A.L., Reama, A., 2017. Real time implementation of backstepping-multiscalar control to induction motor fed by voltage source inverter. Int. J. Hydrogen Energy 42 (28), 17965–17975.

Messalti, S., Gherbi, A., Belkhiat, S., 2013. Improvement of Power System Transient of stability using wind farms based on doubly fed induction generator (DFIG). J. Electr. Eng. 13 (3).

Ouanjli, N.E., Derouich, A., El Ghzizal, A., El Mourabit, Y., Taoussi, M., 2017. Contribution to the improvement of the performances of doubly fed induction machine functioning in motor mode by the DTC control. Intl. J. Power Electron. Drive Syst. 8 (3), 1117–1127.

Ouledali, O., Meroufel, A., Wira, P., Bentouba, S., 2015. Direct torque fuzzy control of PMSM based on SVM. Energy Procedia 74, 1314–1322.

Ourici, A., 2012. Double flux orientation control for a doubly fed induction machine. Int. J. Electr. Power Energy Syst. 43 (1), 617–620.

Panchade, V.M., Chile, R.H., Patre, B.M., 2013. A survey on sliding mode control strategies for induction motors. Annu. Rev. Control 37 (2), 289–307.

Robyns, B., Berthereau, F., Hautier, J.P., Buyse, H., 2000. A fuzzy-logic-based multimodel field orientation in an indirect FOC of an induction motor. IEEE Trans. Ind. Electron. 47 (2), 380–388.

Sutikno, T., Idris, N.R.N., Jidin, A., 2014. A review of direct torque control of induction motors for sustainable reliability and energy efficient drives. Renew. Sustainable Energy Rev. 32, 548–558.

Takahashi, I., Noguchi, T., 1986. A new quick-response and high-efficiency control strategy of an induction motor. IEEE Trans. Ind. Appl. (5), 820–827.

Taoussi, M., Karim, M., Hammoumi, D., El Bekkali, C., Bossoufi, B., El Ouanjli, N., 2017, May. Comparative study between Backstepping adaptive and Field-oriented control of the DFIG applied to wind turbines. In: International Conference in Advanced Technologies for Signal and Image Processing, pp. 1–6.

Telford, D., Dunnigan, M.W., Williams, B.W., 2001. A novel torque-ripple reduction strategy for direct torque control [of induction motor]. IEEE Trans. Ind. Electron. 48 (4), 867–870.

Zemmit, A., Messalti, S., Harrag, A., 2016. Innovative improved direct torque control of doubly fed induction machine (DFIM) using artificial neural network (ANN-DTC). Intl. J. Appl. Eng. Res. 11 (16), 9099–9105.

Zemmit, A., Messalti, S., Harrag, A., 2017. A new improved DTC of doubly fed induction machine using GA-based PI controller. Ain Shams Eng. J.